Pupil Localization Algorithm Combining Convex Area Voting and Model Constraint[1]

Yuanhui Zhang*, Yan Li, Bo Xie, Xiaolu Li, and Junjiang Zhu**

College of Mechanical and Electrical Engineering, China Jiliang University, Zhejiang Hangzhou 310018

**e-mail: zyh@cjlu.edu.cn;*

***e-mail: yannnl@163.com*

Abstract– Locating the center of the eyes plays a significant role in many computer vision applications and research, such as face alignment, face recognition, human-computer interaction, control devices for disabled people, user attention and gaze estimation. The disturbances such as occlusions by eyelashes or eyelids, uneven spots and spectacle frames of glasses affect the accuracy and stability of eye center location. This paper presents a hybrid eye center locating methodology for infrared eye images. The pupil edge points are extracted by Starburst algorithm, and when we get the position and the gradient of the edge points, the approximate pupil boundary is determined by a convex region voting methods. After that, the boundary edge points are iteratively optimized by fitting an ellipses modeling constraint. Finally, the pupil is located correctly. Experiment shows that this algorithm has performance advantages compared with some state of the art approaches in pupil localization accuracy, iteration times and their performance. This algorithm combining convex area voting and model constraint has strong robustness, high accuracy and speed in real environments with occlusions and distortion pupil.

Keywords: infrared image processing, convex area voting, model constraint, gradient feature, outliers eliminate

DOI: 10.1134/S1054661817040216

INTRODUCTION

Eye location and tracking are important tasks in many computer vision applications. Some of the most common examples are the application to face alignment, face recognition, user attention, and gaze (e.g. driving and marketing), and control devices for disabled people [1].

Unfortunately, the common problem of the above techniques is the requirement of intrusive and expensive sensors. For example, in face recognition, difficulties arise from the fact that the face is a changeable social organ displaying a variety of expressions, as well as being an active three-dimensional (3-D) object whose image varies with viewing angle, pose, illumination, accoutrements, and age.

The difficulties mainly come from two sources, the first source is the appearance of the eye image is distorted due to extreme head pose or eye rotations, thus that pupil or iris region does not have a standard circle boundary, while pupil size varies when light changes. The second source comes from various disturbances which includes partial occlusion by eye lashes or eyelids, image noise corruption by uneven illumination or spots by spectacle frames of glasses.

In recent years, many algorithms have been proposed in the study of pupil localization, such as the pupil centering algorithm based on selective threshold inversion and radial symmetry proposed by Zhao Yantao et al. [2], the particle swarm algorithm proposed by Zhang et al., the pupil accurate detection algorithm combined by Hough transform and contour matching proposed by Shunbing Mao et al. [3]. Su Yeong Gwon et al have proposed an algorithm to locate the eye area with Adaboost and SVM and determine the circular pupil center with image binary operation [4]. Roberto Valenti has proposed an accurate algorithm to locate and track the center of eyes using contour feature [5].

Wang Zijing et al. proposed an arc length increment method based on a voting system to locate the center of the pupil [6]. Hu Xu et al. proposed a fast method of pupil and eye location based on gradient feature reconstruction [7].

Above mentioned algorithms can correctly locate center of the undeformed pupil in some kinds of ideal circumstances, their robustness is not good in environment of external interference. Above mentioned algorithms can correctly locate the center of the pupil as they assume for simplicity that the pupil are roughly circular. To solve the fitting problem of deformed pupil in the eye image, Daugman's algorithm based on Fourier series can locate the deformed pupil accurately, but it needs a large amount of calculation [8]. Li introduced a localization method based on ellipse model. This method uses close headset system to track

[1]The article is published in the original.

Received June 19, 2017

gaze and locates the pupil by five points RANSAC (random sample consensus) algorithm. Since it fits an ellipse by randomly sampled five points in each iteration, the probabilities of invalid sampling and calculation are increased when noise-signal ratio increases [9]. Based on Li's method, Colombo applied an elliptical constraint to filter out most of the noise points and improved the efficiency and accuracy of the pupil localization. But it still takes long time to calculate the maximum consistent set with large interference due to the inherent property of the RANSAC [10].

In this page, we propose a novel two-stage algorithm to locate the eye center. The first stage convex region voting attempts to remove noise rapidly from various disturbances, the second stage then uses model constraint to handle the deformed pupil issues. More specifically, it starts from extracting the edge points of pupil image with Starburst algorithm [9]. Then, it takes a vote with gradient vector for each edge point. The convex region with high votes is segmented to be the prospect pupil region. The edge points near the convex region boundary are initially used to fit an ellipse pupil model. Finally, it iteratively optimizes the inlier point set with model constraint. The ellipse fitting method is based on algebraic distance [11]. The algorithm can quickly and effectively eliminate outliers and improve the efficiency and accuracy of pupil localization.

Contents of this paper are organized as follows, Section 2 elaborates pupil localization algorithm, Section 3 shows the experimental results and the relevant comparative analysis, and finally, the paper ended by a conclusion section.

CONVEX REGION VOTING AND MODEL CONSTRAINT ALGORITHM

We choose the pupil center as the eye center, as it is stable and has geometry advantage in images than iris center and are commonly used in eye localization based applications [12]. Then our proposed algorithm mainly consists of two stages: inliers extracting based on convex region voting and inliers refinement based on model constraint. The inliers are the pupil edge points, while the outliers refer to the edges points in all others parts of the images, such as the edge points of the spots or eyelids. Before the voting stage, we apply image pre-process operations, which include calculating the position and the gradient of the candidate edge points.

Prospective Pupil Edge Points Extraction

The boundary of the pupil is crucial element to locate the eye center; here feature-based methods are used to extract feature points on this boundary. Figure 1a is an infrared pupil image. Traditional edge detecting algorithms such as Sobel or Canny edge detector are not suitable to eliminate noises, since those detectors are sensitive to the image noise. Figure 1b shows the result of the Sobel edge detector. It extracts many spurious edge points around the eyelid and limbus, although we can apply image filter such as Gaussian filter to the original image, but this could also lose the saliency feature around the pupil to get rid of noise points and correctly detect the pupil contour, we adopt the Starburst algorithm [9]. The algorithm casts search rays outward from an initial seed point assumed to lie within close proximity to the pupil, and then casts back toward the center to generate additional points; Fig. 1c shows the result. Compared with Fig. 1b, Starburst algorithm can effectively remove the noisy points caused by the disturbances, while preserving as much edge points around the pupil boundary as possible. Though noise points are not totally removed by Starburst algorithms, they will be eliminated in further stages.

Inliers Extracting by Convex Region Voting

Li DongHeng's Startburst algorithm uses RANSAC to further eliminates the spurious points, while we choose a voting based algorithm which is already successfully used on grouping Nuclei in Breast Histopathology Images [13]. The main reason is that the pupil region (even deformed pupil) is approximately a convex image object, and once we find all the prospective pupil edge points, we can find the supporting lines (the line orthogonal to the gradient vector) around the convex region, and finally use a voting algorithm to eliminates the noisy feature points. To get all the supporting lines, the gradient vector should be calculated at all the edge points location in Fig. 1c, the result is shown in Fig. 2. The hollow points indicate the edge points, and the arrows are the gradient vectors, large arrow length means there is a strong gradient vector around the edge point. For a point with pixel coordinates (x, y) in the image I, its pixel intensity value is $I(x, y)$, the gradient vector can be constructed by partial derivative of the I on x and y directions. The vector function G is defined as $G(I) = \left[\frac{\partial I}{\partial x}, \frac{\partial I}{\partial y}\right]^T$. The gradient vector always points along the direction of largest change of image intensities. It is tangent to the edge curve and directs from the darkest side to the brightest side.

Voting Process

We first give a simple voting demo image to show how voting process works, and then we show the voting result of the pupil image. The convex region voting algorithm is divided into four steps:

Step 1. Initialize an empty accumulator I' which has the same size of the pupil image I, and all the pixels in the image have initially zero pixel values. The pixel values are used to accumulate the votes.

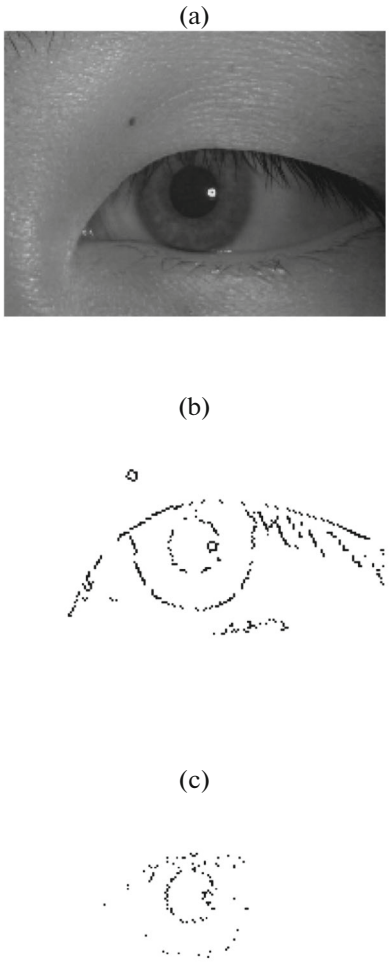

Fig. 1. The result of the extracting edge points with different algorithms. (a) pupil image; (b) the result of the extracting edge points with Sobel algorithm; (c) the result of the extracting edge points with Starburst algorithm.

Step 2. For each gradient vector, find its supporting line. The supporting line simply divides the whole voting image I' into two half-planes. All the pixels in the half-plane where the vector resides keep the same vote value, while all pixels in the other half-plane are increased by one.

The voting rule is depicted by Fig. 3a, the ellipse denotes a simplified pupil, **e** is a gradient vector pointing downward, line l is the convex supporting line. In the upper half-plane, all the pixels have vote value 1, and in the lower half-plane, all the pixels' value remains 0. To determine whether a single pixel need to add 1 or not, we use the inner product of the two vectors. One vector is the gradient vector **e**, the other one is the displacement vector starting from the edge point to the current voting pixel, in Fig. 3a, the **m** and **n** are displacement vectors. In the Fig. 3a, the inner product of **n** and **e** is negative, so the pixel value in accumulator image pointed by **n** should increase by 1, while the product of **m** and **e** is positive, the pixel pointed by **m** remains unchanged. Figure 3b shows the accumulator image of seven edge points vote, the convex region (brightest area in the image) bounded by seven supporting lines has the largest vote value 7, the shape of the region is a convex polygon which approximates to an ellipse. The more gradient vectors used for voting, the region with high votes are more approximating to the pupil area. Figure 3c shows the pixels values of the accumulator image as a 3D surface. The voting process described here is quite similar to the voting scheme used in Hough line detection, where the largest peak values in the accumulator images are the detected Hough lines.

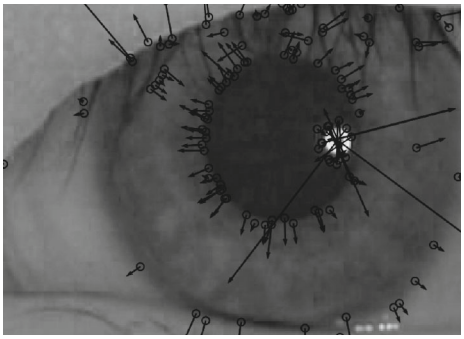

Fig. 2. Gradient vector fields in the pupil image.

Step 3. After applying the voting algorithm on a real pupil image, the accumulator image I' is normalized (we cast the vote value to the range from 0 to 255) and shown in Fig. 4. The accumulator image was plotted in the XY plane, and the 3D surface graph is the vote on each image location. The X and Y axes are the coordinates of the image, the Z axis denotes the normalized vote. The peek in the 3D graph corresponds to the brightest region in the accumulator image in XY plane, which is the pupil region. The approximate pupil region is segmented by Otsu's threshold method. After that, we get the centroid P_c of the extracted pupil region with weighted average method, P_c is calculated by the first moment of the segmented region as the centroid. The votes on the accumulator image caused by noise edges are randomly scattered, so they do not affect the localization of the pupil region.

Step 4. In this step, we try to extract edge points near the pupil boundary, and exclude edge points far from the boundary. We build a data set M whose elements are the distances from the edge points to the centroid point P_c in the extracted convex region. The distance histogram is shown in Fig. 5. Horizontal axis is the distance (length in pixels), the vertical axis is the number of edge points fall in a specific distance bin. We find that the two valleys to the neighborhood of the peak value by balanced histogram algorithm. For example, in the Fig. 5, the two valleys have X coordi-

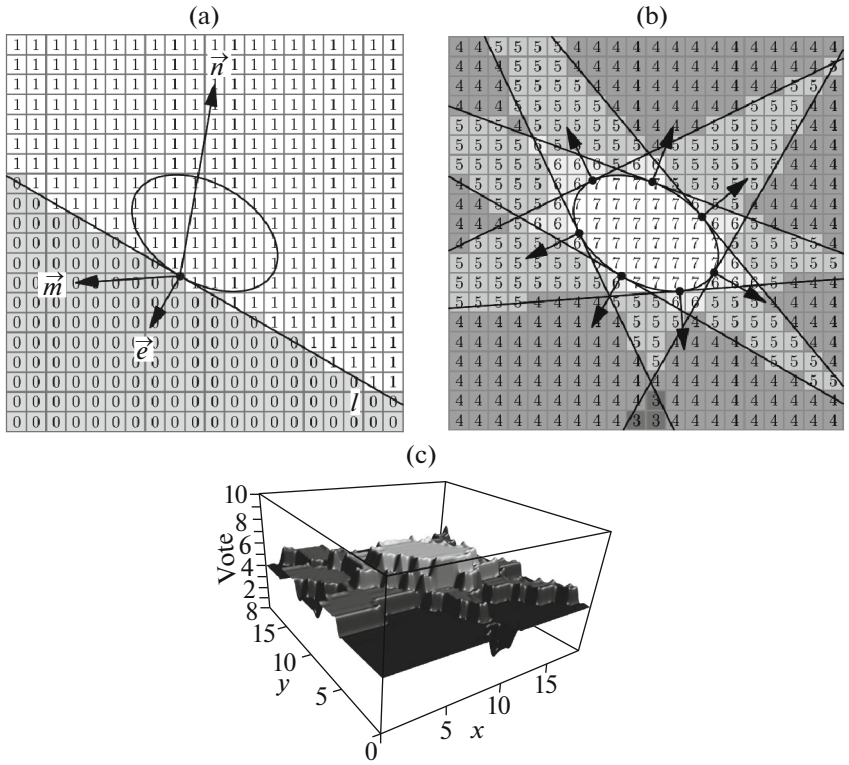

Fig. 3. The accumulator image of convex region voting algorithm. (a) one edge point voting; (b) seven edge points voting; (c) the vote of the accumulator image in 3D view.

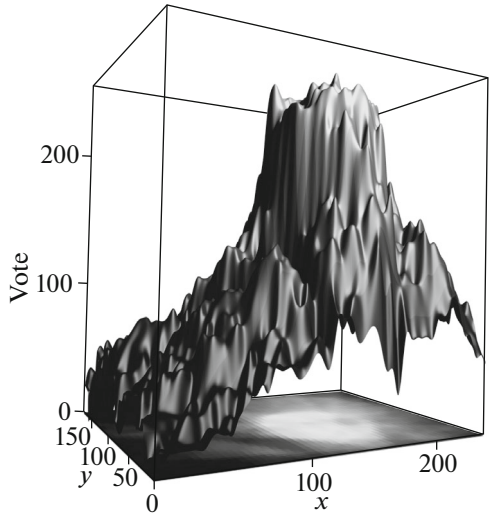

Fig. 4. The normalized accumulator image after convex region voting in 3D view.

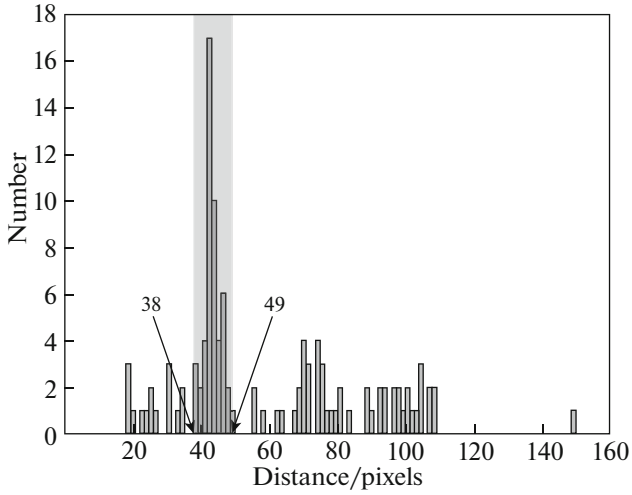

Fig. 5. histogram of distance from edge points to centroid.

nates $R_{in} = 38$ and $R_{out} = 49$. Edge points whose distances to the centroid fall into the interval from 38 to 49 pixels are marked as inliers, other edge points are marked as outliers.

As shown in the Fig. 6, a ring area is drawn, with its center point $\boldsymbol{P}_c$. The ring's inner radius is R_{in} and outer radius is R_{out}. The edge points marked with solid black dots are inliers which are locating inside the ring area, while other edge points marked with hollow dots are outliers.

Inlier Refinement Based on Model Constraint

The convex region voting algorithm can effectively eliminate many outliers, but there are still some noise

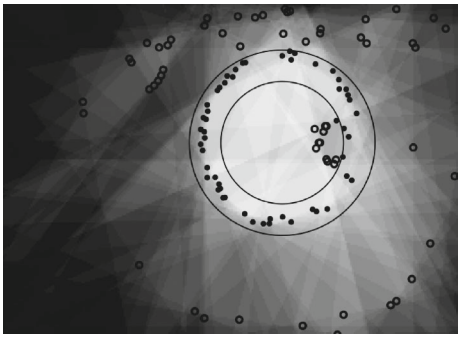

Fig. 6. Inliers extracted based on convex region voting.

points close to the pupil boundary, which are difficult to remove. For example, in Fig. 6, a few points marked with black solid dots on the ring do not belong to the real pupil edge, but these points are incorrectly classified as inliers in the previous voting stage. Therefore, inlier points need to be refined, we use an iterative algorithm based on the model constraint to eliminate outliers of this type. An ellipse model has to be fitted with the current inliers. Then we calculate the average deviation of the model and all the distances from edge points to the model. Further, we iteratively eliminate ones whose distances to the fitted model exceed a threshold. The refinement runes iteratively until the inliers set becomes stable. It can even retrieve misclassified inliers, whose are the true pupil edge points excluded by the previous voting stage. Pseudo-code is listed in Fig. 7.

The inlier points refinement algorithm has following four steps:

Step 1, fit a model E with ellipse fitting method [11] to the inliers selected by the area voting inliers detection algorithm.

Step 2, test all the edge points with respect to E, and classify the edge points whose distances exceed a threshold (we choose three times of the standard deviation as the threshold, but a minimal error is used here to avoid over convergence) as outliers, the remaining edge points are marked as inliers. Update the inliers set. In our experiment, we set the $e = 2$.

Step 3, refit model E based on the updated inliers.

Step 4, repeat step 2 and step 3 until inlier point set gets stable.

Figure 8 shows refined inliers by this stage. Comparing with Fig. 6, the points marked with star in Fig. 8 are edge points newly added into the refined inlier set. The points marked with triangle are edge points removed from the inlier set after the inliers refinement.

The final inliers are used to compute pupil localization with the ellipse fitting method after convex region voting and model constraint. Figure 9 visualizes the result; the white ellipse is the final estimated outline of pupil, thus the center of the ellipse is the pupil center.

Input1 : A $\{(x_i, y_i)\}_{i\in \mathrm{I}}$ is the edge point set of size I

Input2 : B:$\{(x_i, y_i)\}_{i\in l}$ is the initial inlier point set of size l

Output : C is the final refined inlier point set

1. Initialize : $\mathrm{B}' \leftarrow \mathrm{A}, \mathrm{B} \leftarrow null$
2. *while*$(\mathrm{B} \neq \mathrm{B}')$ do
3. $\mathrm{B} \leftarrow \mathrm{B}'$
4. fit an ellipse model E on set B : $f(x_i, y_i) = 0$ to $\{(x_i, y_i)\}_{i\in l}$
5. compute average fitting deviation $\sigma = \sqrt{\frac{1}{|l|}\sum_{i\in l} f^2(x_i, y_i)}$
6. $e = \min(3\sigma,$ minimal error$)$
7. $\mathrm{B}' \leftarrow \{i : f(x_i, y_i) < e\}_{i\in \mathrm{I}}$
8. *end* while
9. return : $\mathrm{C} \leftarrow \mathrm{B}$

Fig. 7. Pseudo-code of inlier points refinement algorithm based on the model constraint.

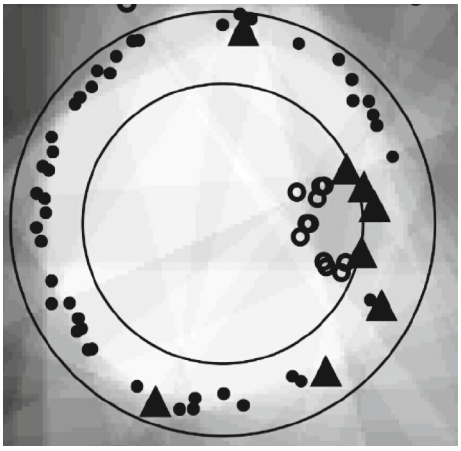

Fig. 8. Inliers refinement based on model constraint.

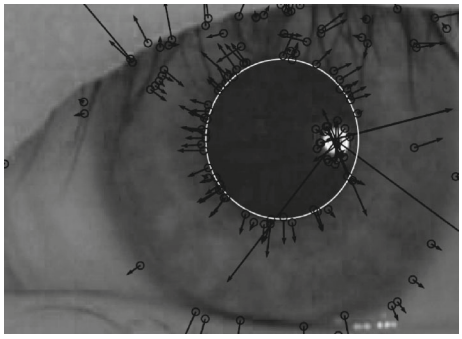

Fig. 9. The result of the pupil localization.

EXPERIMENTAL RESULTS AND ANALYSIS

Experimental Data and Evaluation Method

An evaluation is made on images from the Iris Image Database Version 4.0 released by CASIA (Center for Biometrics and Security Research of Chinese Academy of Sciences). The image database contains images from CASIA-Iris-Thousand, CASIA-Iris-Syn, CASIA-Iris-Lamp, CASIA-Iris-Twins four groups, 200 images are used in our tests. The image size is 640×480 pixels, and the types of interference are different luminance, undesired reflection, eyelashes, eyeglass frame and eye motion blurring. The test program was written in C++ language, and is based on OpenCV library. An Intel Core-i5 3.3G Hz CPU with 4Gb memory is used for running the tests. Since it is hard to find the true pupil center in the image, we have manually calibrated. The center and corner parameter of the eye manually calibrated are treated as the experimental standard values. The normalized error is adopted as the accuracy measure for the found eye locations. It is defined as: $e = \frac{d}{w}$, where the d is the Euclidean distance between the pupil center calculated and manually calibrated, and w is the Euclidean distance between the inner and outer corners of the eye manually calibrated. In our measure, smaller normalized error means more accurate localization result. After the experiment, we list the percentages of images their normalized errors is less than 4 and 10%.

Experimental Comparison

To verify the efficiency of proposed strategy, the experiments have been made by comparing three other methods in the fields. Those methods include pupil localization method based on Invariant Isocentric Patterns (IIP) [5], the method combing RANSAC and ellipse constraint (REC) [10], and the mean of the gradient (MOG) [14]. Our proposed method shares the image preprocessing stage on the original image with REC to get candidate edge points by Starburst algorithm. Pupil localization accuracy, iteration times and their performance are compared. The results are listed in the table. The left part of the table contains results of normal pupil images, and the right part shows results with eye images containing several kinds of interferences. In the column labeled "time (ms)", we list two time components used in two stages (convex region voting and model constraint) separately, so the total time of our proposed method are their summation.

Table shows that MOG's accuracy decreased dramatically from a performance of 81.82% for e≤4% to a performance of 59.49% for e≤10% when image has inferences. Further investigation shows that when inferences contains some non-circular black blobs, the gradient vectors is largely attracted, then the result is

Table 1. Experimental comparison

Method	Eye image without disturbance			Eye image with disturbance		
	iteration times	time(ms)	Accuracy(%) (e < 4%/10%)	iteration times	time(ms)	Accuracy(%) (e < 4%/10%)
IIP	0	20.3	92.60/100	0	42.2	82.67/92.94
MOG	0	22.8	72.00/98.12	0	14.1	59.49/81.82
REC	11	69.4	92.45/100	25	170.5	84.87/93.73
Proposed	5	4.0+1.2	96.30/100	5	8.4+0.8	90.61/94.26

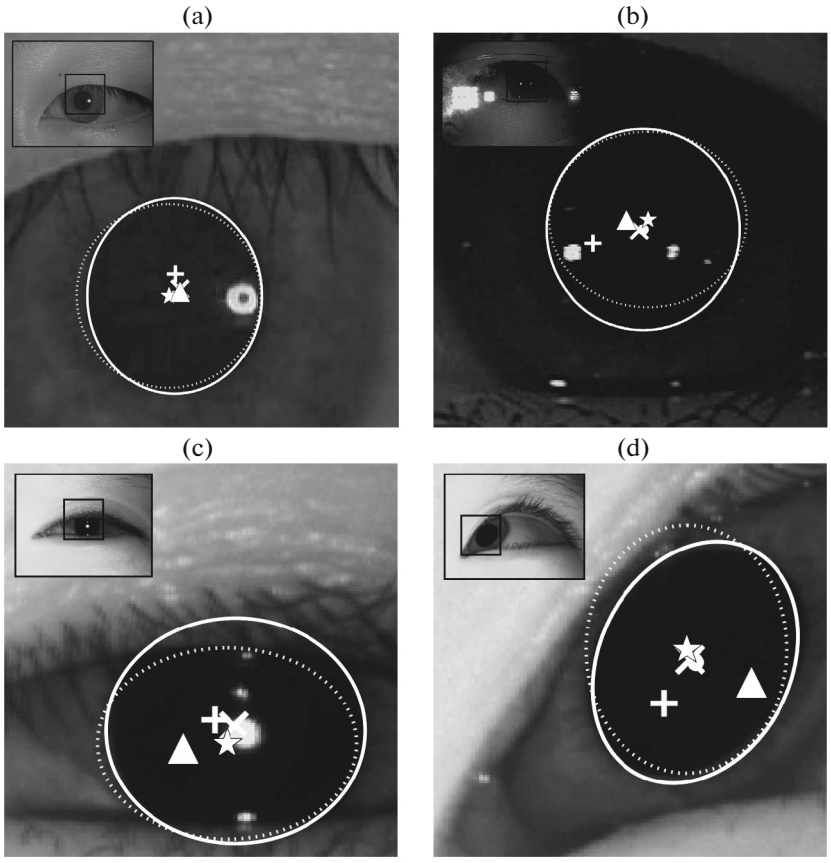

Fig. 10. Experimental comparison of four methods with different disturbances. The calibrated pupil center is marked as a cross symbol, the result of IIP is marked with plus sign, while MOG is marked with triangle, and REC is marked with star (contour as dotted ellipse), and the result of our proposed method are solid dot (contour as solid ellipse). Each image is a sub region of the whole eye image demonstrated in its top left corner. (a) pupil image without disturbance, (b) pupil image with glasses reflection, (c) pupil image with shield, (d) pupil image with the distortion.

far from the real pupil. So, MOG is sensitive on noise from gradient. IIP partially solved this issue by using gradient and curvature, besides that, it sets threshold on radius of edge curvatures and only meaningful parts of the curvatures are used. Both the MOG and IIP use accumulated images to hold the votes, and then pick the peak vote location as pupil center directly. While the REC and our proposed method utilize selectively edges to fit an ellipse, and locate the pupil as ellipse center, thus the latter two are more robust to image distortion, such as if the pupil image is captured from the side view of the head. Figure 10 shows comparing result of four different pupil localization methods. It shows that our proposed method behaves quite well in location accuracy. Especially, when the disturbances occur, the accuracy of the REC and MOG method decrease significantly and their centers are far from the point manually calibrated, only the IIP and our method can locate the center close to the point manually calibrated and remain the higher accuracy, which explains the robustness of our algorithm.

In addition, our proposed method has highest performance among all the four methods. In fact, each method uses some kinds of iterative calculations. IIP and MOG need to iterate through all the pixels of the image to find the estimated pupil center. Its computation complexity is $O(n^2)$ where n is the size of the image. So we rescaled the original image to 160×120 before applying the IIP and MOG, this doesn't decrease the accuracy much compared with the original image but massively reduce the computing time. On the other hand, REC and our proposed methods only need to iterate on the edge points from the Starburst algorithm. But in our method, most of the valid inliers have been classified by convex region voting stage, thus the initial iteration of the model is already close enough to the true pupil model. The RANSAC in REC method take randomly samples from all the edge points set, and takes much time to converge.

Although REC is a robust model based algorithm, it has slow performance for pupil images with large disturbances and does not meet the real-time requirements of gaze positioning system because of the inherent property of the RANSAC. For example, a edge point data set including a number of noise points, it

assumes that the probability of randomly sampling non-noise point from the data set is w. If estimation of model parameters needs k samples (usually, k is the number of the minimum sample required to fit a model), the probability of obtaining an effective model parameter after s samples is $p = 1 - (1 - w^k)^s$ [15]. If a relatively large number of noise points are in the pupil image and w is small, in order to obtain a larger value of p, s should be sufficiently large due to the exponential relationship between k and s. Now, if the rate of interference points is large, for example $w =$ 50%, which means that half of all the edge points in pupil images are noise points, it needs $s = 146$ samples to make the p up to 0.99. To fit the partial pupil contour under occlusion, w becomes smaller, and more samples are needed to calculate the model parameter. Although add the ellipse constraints when need samples, the computation of this algorithm is still too large compared with our proposed method.

CONCLUSION

The pupil localization algorithm based on area voting and model constraint is proposed, it has some improvements from the traditional algorithms, which only use the location information of the feature points to locate the pupil. We utilize both the location information and gradient information of edge points to remove noise points. This means the proposed method mines more information from the image. The algorithm can effectively remove outliers caused by interference in the pupil image; quickly and accurately locate the pupil. Accuracy and stability of gaze point localization are guaranteed. Experimental results show that our algorithm has certain advantages in robustness and speed. Further research could focus on how to accelerate the voting process in order to improve the performance of the algorithm.

ACKNOWLEDGMENTS

This work is supported by the National Natural Science Foundation of China (61302191) and Zhejiang Public Interest Research industrial projects (2016C31112).

REFERENCES

1. C. Jin and Y. Li, "Estimation method of the fixation point in gaze tracking system," Sci. Technol. Eng. **16** (13), 201–205 (2016).
2. Y. Zhao, X. Nie, and J. Luo, "Pupil center location based on radial symmetry combined with selective threshold," J. Optoelectron.·Laser. **27** (11), 1208–1213 (2016).
3. S. Mao, "Exact pupil detection algorithm combining Hough transformation and contour maching," J. Comput. Appl. **36** (5), 1415–1420 (2016).
4. S. Y. Gwon, C. W. Cho, H. C. Lee, W. O. Lee, and K. R. Park, "Robust eye and pupil detection method for gaze tracking," Int. J. Adv. Robotic Syst. **10**, 1–7 (2013).
5. R. Valenti and T. Gevers, "Accurate eye center location through invariant isocentric patterns," IEEE Trans. Pattern Anal. Mach. Intell. **34** (9), 1785–1798 (2012).
6. Z. Wang, H. Chen, and B. Chen, "Pupil positioning approach under low contrast blurred environment," Comput. Eng. Appl. **52** (12), 205–209 (2016).
7. X. Hu and Z. Wang, "Fast eye center and corner location by gradient feature reconstruction," J. Comput.-Aided Design Comput. Graph. **27** (12), 2256–2263 (2015).
8. J. Daugman, "New methods in iris recognition," IEEE Trans. Syst. Man. Cybern. B. Cybern. **37** (5), 1167–1175 (2007).
9. D. Li and D. Winfield, "Starburst: a hybrid algorithm for video-based eye tracking combining feature-based and model-based approaches," in *Proc. IEEE Computer Society Conf. on Computer Vision and Pattern Recognition* (San Diego, 2005), pp. 79–87.
10. C. Colombo, D. Comanducci, and A. Del Bimbo, "Robust tracking and remapping of eye appearance with passive computer vision," ACM Trans. Multimed. Comput. Commun. Appl. **3** (4), 1–20 (2007).
11. R. Halir and J. Flusser, "Numerically stable direct least squares fitting of ellipses," in *Proc. 6th Int. Conf. in Central Europe on Computer Graphics and Visualization* (Plzen, 1998), pp. 59–108.
12. J. Daugman, "How iris recognition works," IEEE Trans. Circuits Syst. Video Technol. **14** (1), 33–36 (2004).
13. M. Paramanandam, et al., "Boundary extraction for imperfectly segmented nuclei in breast histopathology images–a convex edge grouping approach," in *Proc. Int. Workshop on Combinatorial Image Analysis* (Springer Int. Publ., 2014).
14. F. Timm and E. Barth, "Accurate eye center localisation by means of gradients," in *Proc. 6th Int. Conf. on Computer Vision Theory and Applications VISAPP 2011* (Vilamoura, March 5–7, 2011), pp. 125–130.
15. R. Hartley and A. Zisserman, *Multiple View Geometry in Computer Vision* (Cambridge Univ. Press, 2003).

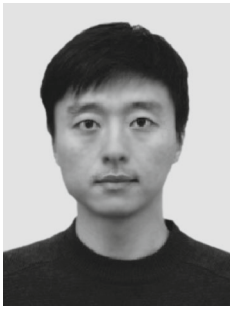

Yuanhui Zhang was born in 1982. He is now working at China Jiliang university as an associate professor. He is also a deputy director of department of Mechanical Engineering. He obtained the bachelor degree from Zhejiang University in 2004. And he got his doctor degree in Zhejiang University in 2011. His research interests include computer vision and robotics. He has had 8 papers published.

Yan Li was born in 1993. She is studying for a master's degree at China Jiliang University and she received the bachelor's degree at the same university in 2015. Her research interests include computer vision and image processing.

Xiaolu Li was born in 1968. He received the bachelor's degree in engineering in 1991 at Shenyang Aeronautics Industrial College and received the master's degree in engineering in 1996 at Zhejiang University. He got his Ph.D. degree in 2005 at Shanghai Jiaotong University. Now he is working at College of Electrical and Mechanical Engineering of China Jiliang University in Hangzhou. His research field is mechatronics design and system simulation and has now had 85 scientific publications.

Bo Xie was born in 1988. He received the bachelor's degree at Shenyang Aeronautics Industrial College in 2013 and received the master's degree at China Jiliang University in 2016. Now his research field is pattern recognition and image processing.

Jun Jiang Zhu was born in 1987. He is now working at China Jiliang university as a lecturer. He obtained the bachelor degree from Zhengzhou University in 2009. And he got his master degree and doctor degree in Hua Zhong University of Science and Technology in China in 2011 and 2015 respectively. Now his research field is signal processing. He has now had 8 papers published, two of which are indexed by SCI.